Reduction of the Titanium Niobium Oxides. I. $TiNb_2O_7$ and $Ti_2Nb_{10}O_{29}$

S. K. E. FORGHANY* AND J. S. ANDERSON†

Inorganic Chemistry Laboratory, University of Oxford, Oxford, United Kingdom

Reduction of the titanium–niobium oxides follows a common pattern. TiO_2 is eliminated, to form a new phase richer in titanium than the original compound, and Nb(iv) replaces Ti(iv) in the original block structure, which is thereby enriched in niobium. With $TiNb_2O_7$, the second phase is a TiO_2–NbO_2 solid solution, with the rutile structure, initially with a high titanium content, in equilibrium with a solid solution of composition Me_3O_7, isostructural with $TiNb_2O_7$. At log p_{O_2} (atm) about -9.0 this reaches the limiting composition $Ti_{0.72}Nb_{2.28}O_7$, in equilibrium with $Ti_{0.56}Nb_{0.44}O_2$. The Me_3O_7 block structure then transforms into the $Me_{12}O_{29}$ block structure ($Ti_2Nb_{10}O_{29}$–$Nb_{12}O_{29}$ solid solution), which rapidly increases in niobium content as reduction continues. Reduction of $Ti_2Nb_{10}O_{29}$ at oxygen fugacities above log p_{O_2} (atm) = -9.0 forms the Me_3O_7 phase as the titanium-rich phase. At log p_{O_2} = -9.0, and a composition about $Ti_{1.6}Nb_{10.4}O_{29}$, the rutile solid solution takes over as second phase. The niobium/titanium ratio in both phases rises as reduction proceeds, and the last vestiges of the $Me_{12}O_{29}$ phase, in equilibrium with the final product, $Ti_{0.17}Nb_{0.67}O_2$, are almost denuded of titanium.

In their systematic equilibrium study of the TiO_2–Nb_2O_5 system, Roth and Coughenor (*1*) identified several double oxide phases, which were shown, by later crystallographic work, to have structures of the "block" type (Table I). (*2–5*).

$Ti_2Nb_{10}O_{29}$ and $TiNb_{24}O_{62}$ are isostructural with the binary, mixed-valence oxides $Nb_{12}O_{29}$ and $Nb_{25}O_{62}$ respectively, and it can be assumed that a complete range of solid solutions should be possible in each case. $TiNb_2O_7$ has no known analog in the binary system, though Eror and Smyth (*6*) found some evidence that Nb(iv) might partially replace Ti(iv) in the structure. Gruehn's careful analytical and phase studies (*7*), together with the thermodynamic equilibrium measurements by Kimura (*8*) and by Schafer *et al.* (*9*) clearly established that H-Nb_2O_5 has a measurable stoichiometric range, on the metal-excess side, at 1300–1400°C, and Gruehn has stated that Ti(iv) can substitute for Nb(iv) in the substoichiometric H-Nb_2O_5.

If the Me^{4+}/Me^{4+} ratio is progressively increased, by reducing any of these Ti–Nb oxides, it is evident that some structural changes must be imposed. Since the reduction of Nb(v) to Nb(iv) is much more facile than that of Ti(iv) to Ti(iii), the ultimate product must be a phase or phases in the TiO_2–NbO_2 system, except at extremely low oxygen fugacities. It is less easy to foresee how the limited number of basic

* Present address: Tussenafdeling der Metaalkunde, Technische Hogeschool, Rotterdamseweg 137, Delft, The Netherlands.
† Present address: Research School of Chemistry, Australian National University, P.O. Box 4, Canberra, A.C.T. 2600, Australia.

TABLE I

	Me(iv)/Me(v) ratio	Unit cell formula	Block structure type
TiO$_2$·Nb$_2$O$_5$	1:2	Ti$_2$Nb$_6$O$_{21}$	$(3 \times 3)_\infty$
2TiO$_2$·5Nb$_2$O$_5$	1:5	Ti$_2$Nb$_{10}$O$_{29}$	$(4 \times 3)_\infty$
TiO$_2$·12Nb$_2$O$_5$	1:12	TiNb$_{24}$O$_{62}$	$(4 \times 3)_s$

block structure types, the possibilities of coherent intergrowth and the formation of Ti(iv)–Nb(iv) solid solutions will control the succession of phases traversed during the reduction.

To obtain equilibrium data, the reaction must be studied at a sufficiently high temperature. Reduction takes place readily below 1000°C in the binary system Nb$_2$O$_5$–NbO$_2$, but coherent intergrowth produces quasi-bivariant phases, with Wadsley-defect intergrowths of the lower block structures; only at the limiting composition Nb$_{12}$O$_{29}$ is an ordered phase produced (10). Kimura argued that the variable equilibrium compositions were due to point defects, rather than to Wadsley defects, but electron microscopy by Iijima (11) and numerous observations in our own laboratory have shown that Wadsley defects are indeed present. Some degree of metal excess nonstoichiometry could, however, be the outcome of overfilling the channels containing tetrahedral sites, as in "GeO$_2$ · 9Nb$_2$O$_5$" (12, 13).

These considerations about the binary system are relevant for the ternary system TiO$_2$–NbO$_2$–Nb$_2$O$_5$, which we have studied at 1400°C. We discuss here the phase equilibria concerned in the reduction of TiNb$_2$O$_7$ and Ti$_2$Nb$_{10}$O$_{29}$; the rather less simple case of TiNb$_{24}$O$_{62}$ is considered in another paper. Common to all the reductions is that a phase richer in TiO$_2$ is eliminated, while the original block structure compound, progressively enriched in niobium, changes through a succession of structures.

Experimental

Materials

Twenty-gram samples of TiNb$_2$O$_7$ and Ti$_2$Nb$_{10}$O$_{29}$ were prepared from high-purity TiO$_2$ and Nb$_2$O$_5$ (Johnson Matthey Specpure). These were weighed out in the exact molar ratios and mixed first in an agate mortar and then in an agate ball mill. The mixtures were pelleted and fired at 1400°C, in platinum crucibles. After 24 hr, the samples were cooled, ground up as before, repelleted and again fired at 1400°. Each sample received 10 such heatings. The products were homogeneous and well ordered, as was checked by X-ray diffraction, electron diffraction, and high-resolution electron microscopy.

To provide a reference material for the TiO$_2$–NbO$_2$ rutile phase, a sample of Ti$_{0.5}$Nb$_{0.5}$O$_2$ was prepared. NbO$_2$ was obtained by reducing Specpure Nb$_2$O$_5$ in hydrogen at 1400°C for 10 hr; it was analyzed by reoxidation to Nb$_2$O$_5$ on a Cahn microbalance. An exactly equimolar mixture of this material with TiO$_2$ was mixed and pelleted as before, and heated at 1100°C for 24 hr in an evacuated silica tube; mixing, pelleting and heating were twice repeated. Its X-ray diffraction pattern indexed with the cell dimensions reported by Marinder et al. (14). Under the conditions of their high-temperature preparation, Marinder and Magneli (15) found the ideal tetragonal rutile structure over a very wide range of composition in the Ti$_{1-x}$Nb$_x$O$_2$ system, without evidence for the TiNb$_2$O$_6$ trirutile structure. Sakata (16) placed the limit of the rutile solid solution at Ti$_{0.15}$Nb$_{0.85}$O$_2$ and in the present discussion, results will be interpreted on the basis of that wide solubility range. Complete reduction of TiNb$_2$O$_7$ and Ti$_2$Nb$_{10}$O$_{29}$ should give rutile phases with the compositions Ti$_{0.33}$Nb$_{0.67}$O$_2$ and Ti$_{0.17}$Nb$_{0.83}$O$_2$, respectively.

Reduction Equilibria

Materials were equilibrated at 1400°C with CO/CO_2 buffers. Preliminary experiments showed that a constant composition was usually reached in about 1 hr; to allow for the much slower processes of ordering and true phase equilibration, samples were kept under equilibrium conditions for much longer periods, up to 10 hr.

In each experiment, about 400 mg of double oxide, in a platinum boat, was reduced in a furnace that permitted rapid quenching, either *in vacuo* or under controlled atmosphere. This furnace will be described elsewhere. In brief, by suitable manipulation of the connections to the gas flow line and to vacuum, the boat could be instantaneously withdrawn from the hot zone of the mullite furnace tube into the cold end. Quenching from reaction temperatures occurred in a few seconds, and to room temperature within a minute.

For the buffer mixtures, CO and CO_2 were purified by molecular sieves and their flow was measured by calibrated flow meters. A steady flow rate of 30 ml/min was maintained during reduction.

Characterization of Reduction Products—Composition

Oxygen/total metal ratios in the reduced, equilibrated materials were determined gravimetrically, by reoxidation to TiO_2 and Nb_2O_5. One hundred-milligram samples were oxidized in air at 1000°C, on a Cahn RG4 thermobalance. The reaction was rapid, constant weight being attained within 1 hr, but heating was continued for 3 hr.

The precision of any one determination of the oxygen/metal ratio x in $(Ti, Nb)O_x$, is estimated to be about ±0.001. The accuracy with which the actual equilibria were measured is less easily assessed, involving as it does the completeness of equilibration, the measurement of buffer gas ratios and their constancy over long periods. From an examination of the results of our own duplicate runs at the same (or very close) nominal buffer gas ratios, and from scrutiny of Kimura's results, it appears that the oxygen fugacity is known to about ±0.05 in log p_{O_2} (atm) and that equilibrium compositions are reliable to about ±0.002.

Phase Analysis

Diffraction patterns were recorded for each sample, using a Hagg–Guinier camera with monochromatized Cu$K\alpha$ radiation. The dominant structures at each composition were thus identified, although uncertainties can arise in identifying the components in mixtures of block structures. The first appearance of any new phase was less certainly determined. The rutile phase was not detectable with high sensitivity in these mixtures and, in these particular systems, the possibility of coherent intergrowth between different structures, as Wadsley defects or as small domains, militates against detecting the first formation of a new block structure. Transitions from one phase field to another could be bracketed, but not directly located with certainty.

The cell dimensions of the rutile phase were measured from the Guinier films, and the corresponding compositions were interpolated from the data recorded by Marinder *et al.* (*14*) for the TiO_2–NbO_2 system. Although this could be done for materials with a fair proportion of the rutile phase, it was not practicable during the early stages of reduction, when weak rutile lines were overlaid by the complex diffraction patterns of the block structures.

Some aspects of the microstructure of the reduced materials, as found from high resolution electron microscopy, will be considered in another paper.

Results

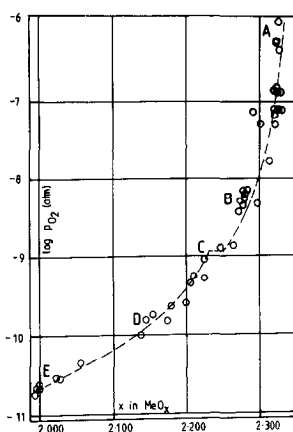Figures 1 and 2 show how the total composition of the reduced materials varies

FIG. 1. Oxygen/metal ratio in reduced TiNb$_2$O$_7$ as a function of the equilibrium oxygen pressure.

FIG. 2. Oxygen/metal ratio in reduced Ti$_2$Nb$_{10}$O$_{29}$ as a function of the equilibrium oxygen pressure.

with the equilibrium oxygen pressure, for TiNb$_2$O$_7$ and Ti$_2$Nb$_{10}$O$_{29}$, respectively. The equilibrium curve for TiNb$_2$O$_7$ has three parts: in the initial stages of reduction, along A–B, the solid phase composition is not strongly dependent upon log p_{O_2}; in the final stages, along D–E, it is strongly dependent, and these segments could be smoothly joined along B–C–D. This might be interpreted as the equilibrium curve of a bivariant system, but fuller consideration of the evidence indicates that there must be a univariant step at some point, narrow enough to be masked by the spacing and the scatter of the experimental points. The probable location of this step is marked at
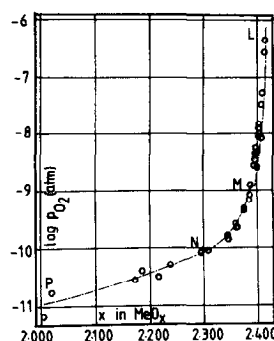
C. Diffraction patterns showed that the material was biphasic along A–B, one constituent being a block structure phase isostructural with TiNb$_2$O$_7$. This Me_3O$_7$ phase (Me = Ti + Nb) persisted down to the point B, i.e., to a total composition $MeO_{2.27}$; from C onward (i.e., for $MeO_{2.24}$ and reduction products poorer in oxygen) the only detectable block structure phase was isostructural with Ti$_2$Nb$_{10}$O$_{29}$.

The second phase, present throughout, had the rutile structure of a Ti$_{1-x}$Nb$_x$O$_2$ solid solution. It changed progressively in composition as reduction continued, as is shown in Table II. It was not practicable to make accurate measurements of the rutile cell along the segment A–B, but at B the phase was approximately Ti$_{0.67}$Nb$_{0.33}$O$_2$, and it became increasingly enriched in

TABLE II

log p_{O_2}	Coexisting phases (mols per mol of TiNb$_2$O$_7$ or Ti$_2$Nb$_{10}$O$_{29}$ starting material)	Oxygen atoms lost	x in MeO_x
−7.0	0.18(Ti$_{0.81}$Nb$_{0.19}$O$_2$) + 0.94(Ti$_{0.92}$Nb$_{2.09}$O$_7$)	−0.06$_1$	2.313
−8.0	0.35(Ti$_{0.72}$Nb$_{0.28}$O$_2$) + 0.88(Ti$_{0.85}$Nb$_{2.15}$O$_7$)	−0.11$_5$	2.295
−8.5	0.55(Ti$_{0.64}$Nb$_{0.36}$O$_2$) + 0.82(Ti$_{0.79}$Nb$_{2.21}$O$_7$)	−0.18$_4$	2.272
−8.83	0.78(Ti$_{0.58}$Nb$_{0.42}$O$_2$) + 0.74(Ti$_{0.73}$Nb$_{2.27}$O$_7$)	−0.26$_1$	2.246
−9.0	0.87(Ti$_{0.56}$Nb$_{0.44}$O$_2$) + 0.71(Ti$_{0.72}$Nb$_{2.28}$O$_2$)	−0.28$_9$	2.244
	0.89(Ti$_{0.56}$Nb$_{0.44}$O$_2$) + 0.93(Ti$_{1.62}$Nb$_{10.38}$O$_{29}$)[a]	−0.35$_8$	2.387[a]
−9.62	1.53(Ti$_{0.46}$Nb$_{0.54}$O$_2$) + 0.87(Ti$_{1.48}$Nb$_{10.52}$O$_{29}$)[a]	−0.644	2.363[a]
−10.0	2.30(Ti$_{0.41}$Nb$_{0.59}$O$_2$) + 0.06(Ti$_{0.96}$Nb$_{11.04}$O$_{29}$)	−0.712	2.122
	3.16(Ti$_{0.41}$Nb$_{0.59}$O$_2$) + 0.74(Ti$_{0.96}$Nb$_{11.04}$O$_{29}$)[a]	−1.30$_9$	2.307[a]
−10.25	5.15(Ti$_{0.37}$Nb$_{0.63}$O$_2$) + 0.57(Ti$_{0.16}$Nb$_{11.84}$O$_{29}$)[a]	−2.14$_4$	2.238[a]

[a] Starting material Ti$_2$Nb$_{10}$O$_{29}$.

niobium as reduction proceeded further. To locate the isobaric tie lines in the total equilibrium diagram, the relation between niobium content and equilibrium oxygen pressure could be adequately represented as:

$$x = 0.279 + 0.168(\log p_{O_2} - 8.0)$$
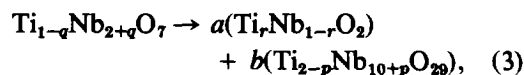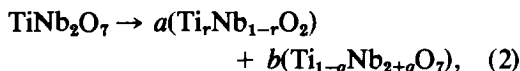$$- 0.0055(\log p_{O_2} - 8.0)^2. \quad (1)$$

The reduction equilibrium curve for $Ti_2Nb_{10}O_{29}$ is similar. Along L–M (Fig. 2), the solid phase composition changed only from $MeO_{2.417}$ to $MeO_{2.39}$ for a drop of three orders of magnitude in $\log p_{O_2}$: in the final stage N–P, the composition changed from $MeO_{2.31}$ to $MeO_{2.00}$ for a small change in oxygen fugacity. As discussed below, this apparently smooth curve, like the reduction curvey of $TiNb_2O_7$, must somewhere contain a univariant step; this evidently has a very narrow compositional breadth, so that it is masked. Its location is indicated by M (Fig. 2). A rutile phase became detectable toward the end of the segment L–M, with a composition close to $Ti_{0.5}Nb_{0.5}O_2$. It rapidly became enriched in niobium as reduction was continued, especially from the point N onward. The product of complete reduction, $Ti_{0.17}Nb_{0.83}O_2$, lies just inside Sakata's reported phase range.
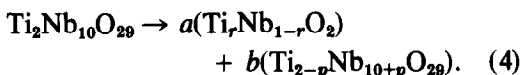
These data suffice to build up the essential features of the equilibrium diagram for the relevant part of the ternary system $NbO_{2.5}$–NbO_2–TiO_2 (Fig. 3). With both $TiNb_2O_7$ and $Ti_2Nb_{10}O_{29}$, the reduction reaction eliminates a rutile phase that is richer in titanium than the starting material. Hence the ratio Nb/Ti in the block structure products must increase progressively during reduction. Reduction of $TiNb_2O_7$ proceeds some way before any new block structure is formed, and this implies that Nb(iv) progressively replaces Ti(iv), to form a phase $Ti_{1-q}Nb_{2+q}O_7$, with the $(3 \times 3)_\infty$ block structure, which can be regarded as a solid solution of $TiNb_2O_7$ with the

hypothetical phase Nb_3O_7. This solid solution has only a limited range of existence, which can be deduced from the equilibrium diagram (see Table II). Beyond that limit, further increase in the Nb/Ti ratio can be accommodated only by transformation to a new structure, namely, the $Me_{12}O_{29}$ structure: a solid solution $Ti_{2-p}Nb_{10+p}O_{29}$ is formed. It follows that the MeO_2 phase, the Me_3O_7 phase and the $Me_{12}O_{29}$ phase must coexist under some conditions, and the equilibrium diagram necessarily contains a univariant three-phase coexistence triangle. That this does not show up in Fig. 1 implies that its compositional breadth, along the trajectory of the reduction reaction, is very narrow. The experimental evidence would fit a value of $\log p_{O_2}$ = about -9.0 for this univariant equilibrium. As reduction is continued, the $Me_{12}O_{29}$ solid solution is both reduced in its turn, and simultaneously enriched in niobium, moving towards the limit of $Nb_{12}O_{29}$.

The first stages in the reduction of $Ti_2Nb_{10}O_{29}$ must be inferred from the equilibrium diagram as a whole, but from the point M onward it involves a bivariant equilibrium between the $Me_{12}O_{29}$ solid solution and the MeO_2 rutile solid solution—i.e., the processes are identically the same as in the later stages of reduction of $TiNb_2O_7$.

The relevant reactions can be expressed in a generalized form. Equation (2) represents the first, bivariant reduction of $TiNb_2O_7$ to the Me_3O_7 solid solution, Eq. (3) the univariant conversion of the Me_3O_7 solid solution to the $Me_{12}O_{29}$ solid solution, and Eq. (4) the bivariant reduction of the $Me_{12}O_{29}$ phase.

$$TiNb_2O_7 \rightarrow a(Ti_rNb_{1-r}O_2)$$
$$+ b(Ti_{1-q}Nb_{2+q}O_7), \quad (2)$$

$$Ti_{1-q}Nb_{2+q}O_7 \rightarrow a(Ti_rNb_{1-r}O_2)$$
$$+ b(Ti_{2-p}Nb_{10+p}O_{29}), \quad (3)$$

$$Ti_2Nb_{10}O_{29} \rightarrow a(Ti_rNb_{1-r}O_2)$$
$$+ b(Ti_{2-p}Nb_{10+p}O_{29}). \quad (4)$$

For known values of the composition of the rutile phase, these mass balance equations should enable the compositions of the coexisting block structures to be calculated at each experimental point. However, quite small experimental uncertainties can result in gross errors and, to overcome this, values for the solid phase compositions that corresponded to given values of log p_{O_2} were interpolated, by smoothing the curves of Figs. 1 and 2, and from Eq. (1). A set of isobaric tie lines, constructed in this way, was consistent with the experimental data, and defined both the three-phase triangle $Me_3O_7-Me_{12}O_{29}-MeO_2$ and the composition range of the Me_3O_7 phase. No high accuracy can be claimed for the resulting compositions, but they must be approximately correct. The univariant equilibrium is undoubtedly established at an oxygen fugacity slightly higher than log $p_{O_2} = -9.0$, and the change of composition, in crossing the three-phase triangle along the reduction trajectory of TiNb$_2$O$_7$ is small—from about $MeO_{2.25}$ to $MeO_{2.23}$—and reconcilable with the data summarized in Fig. 1. Construction of the equilibrium diagram thus fixes the limiting composition of the Me_3O_7 phase as approximately Ti$_{0.75}$Nb$_{2.25}$O$_7$; by analogy with the $Me_{12}O_{29}$ phase, it is drawn as a line phase in Fig. 3, with a negligible range of the oxygen/metal ratio.

The considerations imply, further, that the first stage in the reduction of Ti$_2$Nb$_{10}$O$_{29}$ must involve a bivariant equilibrium with an Me_3O_7 phase enriched in titanium, not with a rutile phase. The reaction can be represented by

$$Ti_2Nb_{10}O_{29} \rightarrow a(Ti_{2-p}Nb_{10+p}O_{29})$$
$$+ b(Ti_{1-q}Nb_{2+q}O_7). \quad (5)$$
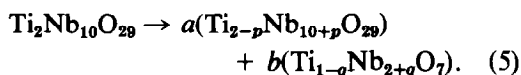
Diffraction patterns of mixed block structures are very complex, and it is difficult to prove directly that (5) fully represents the

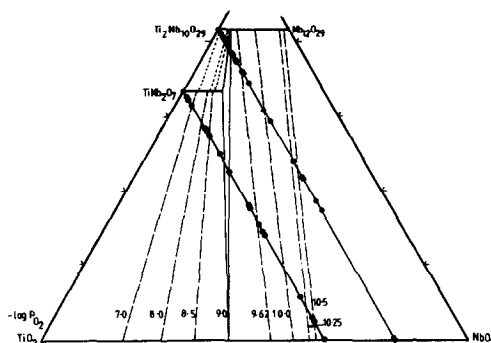FIG. 3. Part of the equilibrium diagram for the ternary system NbO$_{2.5}$-NbO$_2$-TiO$_2$, for oxygen/total metal ratio ≤ 2.417. Reduction trajectories for TiNb$_2$O$_7$ and Ti$_2$Nb$_{10}$O$_{29}$ are shown without all the experimental points. Equilibrium oxygen isobars are optimized to give best fit with experimental results.

initial process, but electron microscope observations (to be reported elsewhere) have disclosed Wadsley defects of the Me_3O_7 structure within the $Me_{12}O_{29}$ structure. The measured data indicate that, at the appearance of the rutile phase, the reduction product consists of 0.73 moles of Ti$_{1.62}$Nb$_{10.38}$O$_{29}$ + 1.07 moles of Ti$_{0.75}$Nb$_{2.25}$O$_7$; the X-ray intensities would be biased in favor of the diffraction pattern from the $Me_{12}O_{29}$ phase. We cannot rule out, however, the possibility that either or both of the Me_3O_7 and the $Me_{12}O_{29}$ phases may have an operationally significant range (in respect of the oxygen/metal ratio), through dissolution of complementary structure elements, in the form of Wadsley defects.

At the other extremity of the reduction trajectory of Ti$_2$Nb$_{10}$O$_{29}$, Kimura's results define the coexistence of Nb$_{12}$O$_{29}$ with NbO$_2$, at log $p_{O_2} = -10.94$. It is evident that as the reduction of the $Me_{12}O_{29}$ phase approaches completion, the rutile solid solution is in equilibrium with a block structure phase that is almost denuded of titanium.

The behavior of these double oxides thus turns upon limitations to the extent to which niobium(iv) and titanium(iv) can replace each other in the family of block structure oxides $mMeO_2 \cdot nNb_2O_5$. When

the limiting composition of the Me_3O_7 phase is reached, during reduction, continued reaction constrains the material to transform into another structure, the $Me_{12}O_{29}$ structure, with a *higher* Nb_2O_5/MeO_2 ratio. This mutual replaceability of niobium(iv) and titanium(iv) is highly structure-specific; it appears to be complete in the $Me_{25}O_{62}$ and $M_{12}O_{29}$ structures, up to about 28 mole% in the Me_3O_7 structure but, as can be inferred from the course of reduction of $TiNb_{24}O_{62}$, to be described in another paper, it can occur to a very small extent, if at all, in the $Nb_{22}O_{54}$ structure.

Acknowledgments

References

1. R. S. Roth and L. W. Coughanour, *J. Res. Nat. Bur. Stand.* **55**, 209 (1955).

2. A. D. Wadsley, *Acta Crystallogr.* **14**, 660, 664 (1961).

3. R. Gruehn and H. Schafer, *Naturwissenschaften* **50**, 642 (1963).

4. R. S. Roth, A. D. Wadsley, and B. M. Gatehouse, *Naturwissenschaften* **51**, 262 (1964).

5. R. S. Roth and A. D. Wadsley, *Acta Crystallogr.* **18**, 724 (1965).

6. N. G. Eror and D. W. Smyth, *in* "Chemistry of Extended Defects in Nonmetallic Solids" (L. Eyring and M. O'Keefe, Eds.), p. 62. North-Holland, Amsterdam (1969).

7. R. Gruehn, N.B.S. Special Publ. 364, Solid State Chemistry 63 (1972).

8. S. Kimura, *J. Solid State Chem.* **6**, 438 (1973).

9. H. Schafer, D. Bergner, and R. Gruehn, *Z. Anorg. Allg. Chem.* **365**, 31 (1969).

10. K. M. Nimmo and J. S. Anderson, *J. Chem. Soc. Dalton Trans.*, 2328 (1972).

11. S. Iijima, S. Kimura, and M. Goto, *Acta Crystallogr. Sect. A* **30**, 251 (1974).

12. J. S. Anderson, D. J. M. Bevan, A. K. Cheetham, R. B. Von Dreele, J. L. Hutchison, and J. Strahle, *Proc. Roy. Soc. A* **346**, 139 (1975).

13. A. J. Skarnulis, S. Iijima, and J. M. Cowley, *Acta Crystallogr. Sect. A* **32**, 799 (1976).

14. B.-O. Marinder, E. Dorm, and M. Seleborg, *Acta Chem. Scand.* **16**, 293 (1962).

15. B.-O. Marinder and A. Magneli, *Acta Chem. Scand.* **12**, 1345 (1958).

16. K. Sakata, *J. Phys. Soc. Japan* **26**, 1067 (1969).